Heat transfer from nanoparticles for targeted destruction of infectious organisms

Michael B. Cortie[a] , David L. Cortie[b] and Victoria Timchenko[c]

[a]*School of Mathematical and Physical Sciences, University of Technology Sydney, Sydney, Australia;* [b]*The Institute for Superconducting and Electronic Materials, University of Wollongong, Wollongong NSW 2522, Australia;* [c]*School of Mechanical and Manufacturing Engineering, University of New South Wales, Sydney, Australia*

CONTACT Michael Cortie [email] Michael.cortie@uts.edu.au [post] School of Mathematical and Physical Sciences, University of Technology Sydney, PO Box 123, Broadway, NSW 2007, Australia

Additional author information

M B Cortie, ORCID ID 0000-0003-3202-6398

D L Cortie, ORCID ID 0000-0003-2383-1619, email: dcortie@uow.edu.au

V. Timchenko, ORCID ID 0000-0002-1228-5344, email: v.timchenko@unsw.edu.au

Table of contents graphic

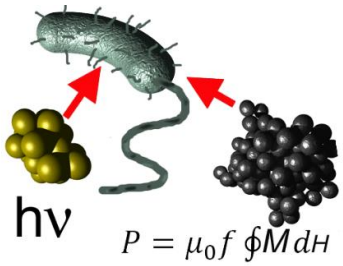

Heat transfer from nanoparticles for targeted destruction of infectious organisms

Whereas the application of optically- or magnetically-heated nanoparticles to destroy tumors is now well-established, the extension of this concept to target pathogens has barely begun. Here we examine the challenge of targeting pathogens by this means and, in particular, explore the issues of power density and heat transfer. Depending on the rate of heating, either hyperthermia or thermoablation may occur. This division of the field is fundamental and implies very different sources of excitation and heat transfer for the two modes, and different strategies for their clinical application. Heating by isolated nanoparticles and by agglomerates of nanoparticles is compared: hyperthermia is much more readily achieved with agglomerates and for large target volumes, a factor which favors magnetic excitation and moderate power densities. In contrast, destruction of planktonic pathogens is best achieved by localized thermoablation and very high power density, a scenario that is best delivered by pulsed optical excitation.

Keywords: hyperthermia; photothermolysis; plasmonic heating; magnetic heating; thermoablation

Introduction

The use of an elevated temperature to destroy pathogens has been on a firm scientific footing since the pioneering work of Louis Pasteur in the mid-Nineteenth Century. However, the industrial process of pasteurization sterilizes almost everything – pathogen or not – in the material that it is applied to. It is only comparatively recently that strategies for selectively applying heat to a specific target cell or organism have been identified. If this can be done efficiently, then destruction would be localized at the position of a target cell or pathogenic organism and collateral damage to the patient's healthy cells would be minimized. Although several strategies have been considered, the idea of targeting a micro- or nanoparticle to the infectious organism, followed by

coupling of an external energy source with the particle, is probably receiving the most attention. Essentially the external source of energy can be light or other electromagnetic radiation, an oscillating magnetic field, ultrasound, or an electric field or current. Depending on the rate and the intensity of the heating, there are two basic outcomes: hyperthermia (increase in local temperature of a few tens of degrees Celsius) and thermoablation. The latter may also involve thermolysis: fragmentation or decomposition of the nanoparticle due to it reaching an extremely high temperature. Of course, if a particle is used then it must be non-toxic, and it should somehow be invisible to the patient's immune system. There are significant challenges in the field [1, 2, 3, 4, 5] but the first clinical use of magnetic hyperthermia has begun [6, 7].

Here we will consider a narrow aspect of the topic: the coupling of the external energy source to the nanoparticles, and the subsequent transfer of heat from them to target organisms. The question that we address is how best to achieve the destruction of pathogens, especially planktonic pathogens, using currently available sources of excitation. Nanoparticles are usually defined as particles in the 1 to 100 nm size range [8]. They are attractive for targeted hyperthermia because they have an ability to penetrate deeply into tissue or organisms. Although heat can also be generated by so-called *fine particles* (which are in the 100 nm to 2500 nm range [8]), we confine our analysis in the present paper to nanoparticles due to their more penetrating nature and the readiness with which they can be chemically functionalized. We do not address the methods by which the nanoparticles can be targeted to the pathogen as this topic has been extensively covered elsewhere. Suffice it to say that there is a variety of active (e.g. antibody functionalization) or passive (e.g. extravasation) targeting schemes that are receiving attention [9] and, for tumors, direct injection is also a possible strategy [1, 2]. However active targeting would be the best method to use against a mobile

infectious organism. We note that most of the nanoparticle/ hyperthermia literature relates to the potential treatment of cancer whereas reports of targeting infectious pathogens this way [10, 11, 12, 13, 14, 15, 16, 17, 18, 19, 20, 21, 22, 23] are relatively scarce. Nevertheless, the physical principles involved in the hyperthermal treatment of either are the same, so the cancer work remains broadly relevant within the framework of the present paper. The main differences are that, in the case of pathogens, there are fewer options for targeting and destruction may require a higher temperature than for cancerous cells [11, 12, 17], thus, as we show here, the optimal power densities required are orders of magnitude greater. Targeting infectious pathogens is, therefore, a comparatively challenging endeavor.

The following sections begin by reviewing mechanisms for energy capture by nanoparticles. We show that light and alternating magnetic fields offer different but complementary opportunities. Next, the heat transfer into surrounding tissue is analyzed and compared for isolated nanoparticles and agglomerates. It is found that extremely high power densities are required to raise isolated nanoparticles to useful temperatures. Special attention is given to the prospect of using gold nanoparticles for hyperthermia via optical excitation. This is due to the special optical properties and chemical nobility of these particles. Finally, merits of optical and magnetic excitation to target pathogens are compared and it is demonstrated that, whereas large tumors can be readily targeted using either light or magnetic fields, planktonic pathogens can only be targeted using light due to the very high power input required.

Energy capture by nanoparticles

Two methods of generating heat in nanoparticles are receiving the bulk of current interest. These are optical excitation and magnetic excitation. The principle behind each

type of excitation will be briefly explained and their use in therapeutic contexts summarized. In addition, it has been reported that heat can also be generated in gold nanoparticles and carbon nanotubes by application of shortwave radiofrequencies [2] or in gold nanoparticles by radiofrequency magnetic induction [24] whilst magnetically-induced mechanical oscillations in suitable particles can also disrupt target cells [25]. Discussion of these other possibilities, however, lies outside of the scope of the present paper.

Optical excitation

Principles

When a photon of light strikes a nanoparticle (or indeed any substance), it may be absorbed, transmitted or scattered. Energy must be conserved so that the total energy of the incoming light equals the sum of the energies of the transmitted, absorbed or scattered light. It is the absorbed light that is converted to heat and hence of interest here. For exploitation of this principle in hyperthermal medicine, the ideal nanoparticle should possess strong absorption at a suitable position in the electromagnetic spectrum, and it should, of course, be biocompatible. Given these constraints, gold nanoparticles are widely believed to be the best candidate for hyperthermia by optical excitation.

Spherical gold nanoparticles undergo an electromagnetic resonance with light which produces a strong absorption peak due to a localized surface plasmon resonance (LSPR). This is at about 520 nm (green light) which corresponds to the middle of the visible range. A relatively low power laser with emission matched to this peak could be a suitable source of energy. Unfortunately, the human body is not particularly transparent to green light so any clinical exploitation of isolated spherical gold nanoparticles is restricted to very shallow depths into tissue.

The optimum range of wavelengths for clinical exploitation of optically-excited heating is 670 to 890 nm, the so-called ‘tissue window’ or ‘NIR window’ [26] but, unfortunately, isolated spherical gold nanoparticles have a negligible optical absorption cross-section over these wavelengths. There are two solutions to this problem. The first is to make use of specialized gold nanoparticles that have shapes with LSPRs that do fall within the tissue window. Gold nanoshells [27] and gold nanorods [28] are probably the best-known examples of these. The relative merits of these two shapes have been explored elsewhere [29, 30]. Other specialized shapes that are also capable of undergoing LSPRs in the tissue window include gold nanocubes, triangles, so-called nano-stars, and similar geometries of lower symmetry. In all cases, the wavelength at which the LSPR occurs can be adjusted by modification of the geometry of the particle. An alternative strategy, but less common, is to use gold nanospheres, but to exploit the red-shifting of their LSPR that occurs when they form closely-packed agglomerates or aggregates [14]. (It is recommended that the term ‘agglomerate’ be used for clusters of nanoparticles that are weakly and reversibly bound by van der Waals or similar secondary bonds, and ‘aggregate’ be used for clusters of nanoparticles that are irreversibly bound together by primary chemical or metallurgical bonds [8].) Either way (whether lower symmetry particle or agglomeration of spheres) significant optical absorption can be developed at wavelengths that are within the tissue window. The LSPR peak associated with such agglomerated entities is broad but this is not a problem in the context of a hyperthermal therapy delivered with a monochromatic light source.

Applications in hyperthermia

Gold nanoshells have received considerable attention in this regard and clinical trials for head and neck tumors, prostate tumors, lung tumors, breast cancer, oropharyngeal

malignancies and acne have been mooted or initiated [2, 31, 32, 33, 34, 35]. However, there have been relatively few recent scientific reports so far on the outcomes of these trials. Preclinical studies involving nanorods are also frequently reported in the scientific literature, again usually with some cancer as the target, for example refs. [36, 37]. As mentioned above, application of these principles to target infectious organisms is far rarer, but, for example, successful *in vitro* trials of the efficacy of gold nanospheres and nanorods against the tachyzoite phase of the protozoan *Toxoplasmosis gondii* [11, 14] or of gold nanospheres against the bacterium *Staphylococcus aureus* [10] have been reported.

Biocompatibility

Gold is the most commonly used material for these types of applications, due to its biocompatibility [32] and good optical properties. In contrast, while silver actually has significantly better optical properties for these types of plasmonic applications, especially in the visible part of the spectrum, it is susceptible to corrosion. The difference in the optical properties of gold and silver reduces as the excitation wavelength lengthens into the tissue window and the near-infrared [38], a factor which also favors the use of gold.

In conclusion, it is evident that gold offers a suitable combination of chemical and optical properties for light-induced hyperthermia.

Magnetic excitation

Principle

Heat may be generated by applying an oscillating magnetic field to either ferromagnetic or superparamagnetic nanoparticles, however there are many advantages to using the

latter [39]. Like gold nanoparticles, the magnetic nanoparticles can be small and penetrating, can be chemically functionalized, and can be modified by control of their geometry. In addition, superparamagnetic nanoparticles also have the property that they can in principle be guided and heated by an external magnetic field, but that their net magnetic moment vanishes when the field is turned off, which is advantageous.

Superparamagnetism is a phenomenon that only occurs for small particles which possess locally ordered spin structure but have a low volume to give the distinctive magnetic properties illustrated in Figure 1, notably a strongly frequency-dependent magnetic response concurrent with the absence of permanent static magnetization. The low volume of a nanoparticle means that the energy barrier separating each of the degenerate magnetic states is small compared to the thermal energy provided by heat. Thus in the absence of an external field, the nanomagnet undergoes Néel relaxation via continuously flip-flopping between the two states with a characteristic relaxation time given by [40]:

$$\tau_N = \tau_0 . exp\left(\frac{\Delta E}{k_B T}\right) \quad (1)$$

The magnetic relaxation time is determined by the size of the energy barrier $\Delta E \sim KV$ that is proportional to the volume of the nanoparticle (V) and the intrinsic crystalline anisotropy of the magnetic crystal lattice (K). For nanoparticles suspended in fluid, Brownian motion of the surrounding fluid introduces additional reorientation pathways, introducing a second form of relaxation:

$$\tau_B = \frac{3\eta V}{k_B T} \quad (2)$$

, involving biological factors, including the dynamic viscosity of the fluid η and the effective hydrodynamic diameter of the nanoparticle after opsonization (V) [41]. According to the equation from Shliomis [42], the total relaxation time is:

$$\tau = \frac{\tau_B \tau_N}{\tau_B + \tau_N} \quad (3)$$

At sufficiently high temperature (above the 'blocking temperature'), the relaxation between the states is so frequent that on average no magnetization appears in a thermalized particle ensemble. It conveniently turns out that many nanosized materials remain in the superparamagnetic state even at room temperature. This unique feature of superparamagnetism accounts for the coexistence of high magnetization with the absence of remnant (permanent net magnetization) because the system undergoes a time-dependent relaxation towards zero average magnetization after the external field is removed. The low mass/high magnetization allows small concentrations of nanoparticles to yield appreciable effects in the body. The absence of permanent magnetism is an advantage because otherwise magnetized particles tend to interact and agglomerate even in the absence of a field due to dipolar interactions, limiting their blood half-life and biomedical applications.

In the presence of an alternating field, magnetic nanoparticles will attempt to align their magnetic moment with the applied field. Associated with this magnetic reversal, there is an energy cost with irreversibilities leading to power dissipation in the form of heat. For hyperthermia, it is important that the magnetic material contains some degree of hysteresis in order to generate heat losses to the AC field. The increase in internal energy is [41, 43]:

$$\Delta U = -\mu_0 \oint M(t) dH \qquad (2)$$

per cycle, where H is the magnetic field intensity, M(t) is the dynamic magnetization, and the integral is performed over a single cycle of the field. Power dissipation at a frequency f is given by

$$P = f.\Delta U = \mu_0 f \oint M(t) dH \qquad (3)$$

The integrated term is proportional to the area enclosed by the M vs H hysteresis curve [40]. For a superparamagnet, this can be related to the out-of-phase dynamic susceptibility and is strongly dependent on the AC frequency because the integral involving M(t) is frequency dependent as it involves the superparamagnetic relaxation processes.

Applications in hyperthermia

Hypothermia or pasteurization using magnetic particles has a long history: the concept was mentioned in a paper by Goldenberg and Tranter in 1952 [44]and tested on tumors in dogs by Gilchrist in 1957 [1]. Renewed interest appeared from the 1980s with numerous groups investigating smaller particles coated for increased biocompatibility. Superparamagnetic iron oxides, Fe_3O_4 and γ-Fe_2O_3, remain the material of choice. Many preclinical studies have shown that positive temperature differences can be induced between tumors and normal tissue, however, there are also reports claiming that useful results can be obtained even if a positive temperature difference cannot be measured, so-called "cold hyperthermia" [5, 45, 46]. This implies a more localized mechanism of action than whole-tumor hyperthermia in these cases.

Despite the widespread preclinical interest, relatively few clinical trials have been reported, so far. The examples known to the authors include investigations of the use of magnetic particles against glioblastoma multiforme, and prostate and pancreatic cancer [5, 47]. Some commercial clinical exploitation has recently begun in the European Union [6].

Biocompatibility

Currently only the iron oxides are approved for human usage because of their known

metabolic pathways. There would be numerous advantages to using more typical ferromagnetic metals such as nickel, cobalt and $Ni_{80}Fe_{20}$ since these materials tend to have higher magnetization. On the other hand, such materials are carcinogenic or toxic, and would need to be insulated from the body by the use of a surface coating of gold or a polymer. While such approaches are certainly feasible, there is no horizon for the approval of such materials in clinical trials.

Methods for analyzing local heating from a nanoparticle

There have been a number or prior studies in which the heat transfer from particles or nanoparticles has been examined (see, for example, refs. [41, 48, 49, 50, 51, 52, 53, 54, 55, 56, 57, 58]. There are, however, many important differences between the assumptions made in these studies and in the scenarios in which clinicians might wish to apply hyperthermia or thermoablation. In the present paper we focus on answering the question of how best to deliver a useful degree of hyperthermia or thermoablation to a pathogen.

In general, the transfer of energy from the heated zone to the surrounding medium may be handled in two ways, either by assuming transfer by conduction or by convection. In the case of photothermolysis, radiative heat transfer could also be considered due to the very high temperatures reached by the particle. Somewhat different analytical forms result, with the assumption of the conduction case generally providing the faster rate of heat transfer since there is no boundary layer to retard heat flow [59].

The temperature of a nanoparticle and the flow of heat outwards into the surrounding fluid or other thermally conductive medium can be modelled using the

analytical expression of Goldenberg and Tranter [44], which, interestingly, was derived in 1952 to support early studies into radiofrequency-assisted pasteurization and sterilization, or it can be modelled by more tractable expressions due to Pustovalov [51]. The latter predict a slightly more rapid rate of heating within the nanoparticle than does the former due to slightly different assumptions having been made in its derivation, however outside of the heated sphere, the temperature distribution of the two solutions is effectively identical. In both cases, the models consider certain biological factors such as the thermal conductivity of the surrounding tissue, bones or fat. On the other hand, certain factors such as vascularization and multiple diffuse interfaces are simplified or ignored, so at best the models provide an upper limit on the heating. It is convenient to use the G&T equations when energy input is expressed in W/m^3 and the Pustovalov ones when energy is expressed in W/m^2 of flux. Both assume conductive heat transfer so are likely to slightly overestimate the cooling rate. In addition, the analytical solution for transient convective heat transfer from a sphere [60] will be used here to estimate cooling after the excitation is terminated.

In the case of optical excitation, the power captured by an isolated nanoparticle that is undergoing a localized plasmon resonance is

$$\dot{Q} = \int_{\lambda_1}^{\lambda_2} C_{abs}(\lambda) E(\lambda) d\lambda \tag{4}$$

where $\dot{Q}$ is the heat transfer rate (watts), $C_{abs}(\lambda)$ the wavelength-dependent absorption cross-section, $E(\lambda)$ is the spectral irradiance of the light source ($W.m^{-2}.nm^{-1}$), and λ_1 and λ_2 (nm) are the limiting wavelengths of light over which the light source operates [54]. $C_{abs}(\lambda)$ is readily available for arbitrary shapes by calculation [61]. For illustrative purposes, a gold nanoparticle of 30 nm diameter will generate 1.4×10^{-9} W when irradiated with a 100 mW laser of 0.5 mm diameter under conditions where $Q_{abs} = 4$.

Modelling the heat capture from the intrinsic magnetic properties of materials, by contrast, is more difficult because of the frequency-dependent susceptibility, and lies outside of the scope of the present paper. Generally, a measured value may be used for first-order estimates; for example data provided in a recent publication [45] may be used to provide an estimate of 5×10^{-13} W per oxide nanoparticle of 66 nm diameter when it is excited in a typically applied magnetic field of 10 kA/m at about 900 kHz.

Finally, a note on the units for power. The excitation power can be expressed in W/m^2 if the particle is considered to lie in an excitation field and have a capture cross-section (in physical units of area) with dimensionless efficiency φ. The captured power may also be parameterized as W/m^3 relative to the active volume that is undergoing excitation. These parameters can be converted into one another by appropriate manipulation. The fluence delivered is obtained by multiplying the power by the time it is applied, and can similarly be presented per unit area or per unit volume, whichever is the more convenient.

Heat transfer to the surrounding tissues: localized pasteurization versus thermoablation

For the purposes of targeting and destroying pathogens via nanoparticle heating, it does not matter whether the energy was initially supplied by optical or magnetic excitation, the end result will be the same provided that the tissue surrounding the target is transparent to the laser wavelength used. In both cases the objective is usually to raise the temperature of the target cell or organism to a level at which apoptosis or direct necrosis occurs while avoiding damage to the surrounding tissue. Temperatures upwards of about 42 °C are required, and of course higher temperatures are better [2]. It is, however, useful to draw a distinction between two rather different modes of action: local pasteurization and thermoablation. In the temperature range 43 to 50°C range,

apoptosis is the likely outcome, but extensive protein denaturing and necrosis will result as temperatures rise towards the boiling point of water. We will group both of these phenomena together here as 'localized pasteurization'. In contrast, in an alternative strategy, the temperature of the nanoparticle is raised so high (>2000°C) that it fragments and generates a steam shockwave, thereby perforating a nearby cell membrane or cell wall by mechanical means [10, 62, 63]. This latter mechanism has been termed 'photothermolysis' [64] if generated by light. Thermolysis can only be achieved by a rate of heating that is so fast that the nanoparticle can effectively be treated as an adiabatic system. Since (as we will see later) heat transfer from particle to environment takes place on a time scale of a few nanoseconds, exploitation of photothermolysis requires that the fluence is delivered in even shorter pulses.

The isolated particle scenario is not particularly effective for local pasteurization as heat transfer out from such a particle is exceedingly rapid which hinders a high local temperature from being achieved [49, 58]. In fact, it is usually much better to deploy a multiplicity of particles to the vicinity of the target cell or organism in order to deliver a lethal dose of thermal energy [52], however the optical properties of agglomerates are quite different from those of individual isolated particles. Therefore, we will divide the discussion below into two threads, corresponding to heating from isolated nanoparticles and from agglomerated clusters of nanoparticles.

Heat generation by isolated nanoparticles

Our analysis does not depend on the source of the applied thermal energy (optical, magnetic etc.) but for simplicity we will use the language appropriate to the case of optical excitation in the discussion that follows.

In broad summary, the local region over which the elevated temperature is obtained is very limited in the case of individual small, spherical heat sources. Some illustrative results of calculations for nanoparticles immersed in water are shown in Figure 2. In Figure 2(a) we show an illustrative calculation for a medium power pulsed excitation (1×10^{9} W/m^2). It should be noted that the volume of surrounding medium that is heated into the hyperthermia range is very small, only 3.1×10^{-5} μm^3 if the threshold temperature is set at 50°C. Isolated particles will be ineffective in this scenario. In contrast, in Figure 2(b) we show the temperature distribution that can be reached when the nanoparticle is excited at a relatively high power, chosen here as 1.6×10^{11} W/m^2 so that the boiling point of gold is attained. There is still a very steep fall in temperature with distance from the nanoparticle, but the volume of surrounding medium that is heated to at least 50°C is much larger, at 128 μm^3. Naturally, this is an example of the thermolysis mode so there will additionally be mechanical damage to nearby cells due to shock and/or physical perforation by gold fragments.

The rate and duration of heating is a very important factor. Consider the case for a plasmonically-heated nanoparticle. When a single photon of the resonant frequency is absorbed by the nanoparticle, it generates a distribution of hot electrons in about 5 fs (5×10^{-15} seconds). The hot electrons couple to the lattice and relax to generate or amplify lattice phonons over the next ~5 ps (5×10^{-12} s). In effect, phonon vibrations are the main manifestation of the kinetic energy that determines the "temperature" of the nanoparticle from the perspective of heat transfer. At this point the heating has been essentially adiabatic, i.e. little energy has been transferred yet to the medium surrounding the nanoparticle. Over the next 10 to 100 ps the heat flows out to the environment and after about 400 ps the nanoparticle temperature is the same as that of its adjacent medium. The only exception will be if the particle is struck by an intense

pulse of coherent photons (for example by a laser), in which case the initial temperature rise may be so high as to vaporize the nanoparticle and thereby cause a photothermolysis shockwave. In contrast, if the intensity of the pulse is low then the small amount of heat delivered is rapidly transferred away into the surrounding medium with little effect. In this case prolonged illumination and/or a high density of nanoparticles is required to achieve localized pasteurization.

Clearly, the only way that *isolated* nanoparticles can be effective *in vivo* is in thermolysis mode. The question then becomes: how many cell membranes or wall perforations are required to cause necrosis? Pitsillides et al.[62] note that a cell's natural repair processes will heal perforations over a time scale of a few minutes. The damage induced by the photothermolysis must accumulate faster than the rate of repair or else it will recover. In addition, different components of a cell (e.g. membrane, nucleus) will have different tolerance to damage. It is important to note that (photo)thermolysis mode can be effective at relatively low energy inputs (of the order of 0.025 to 0.5 J/cm^2 [10, 62, 63, 65]) provided that the laser pulse power is very high. This is because the effect is extremely local and the destructive process is achieved at the nanoscale before the energy is thermally dissipated into the surrounding medium [63]. In contrast, at least 1 J/cm^2 is normally required [65] for slower modes of heating. In general a safety threshold of 0.1 J/cm^2 has been set for medical lasers [63], so clearly the lower fluences associated with photothermolysis are potentially advantageous.

The FDA have imposed limits of ~3 W/kg on heating due to magnetic fields in MRI devices and there is also a view that the product of frequency and alternating magnetic field amplitude should be less than somewhere between 0.5×10^9 and 5×10^9 A-turns/(m.s) in order to prevent stimulation of nerves or undesirable eddy currents [5, 66]. In practice, however, only a few hundred W/g is available from magnetic

nanoparticles anyway using standard AC fields [58, 66] and so the power required to destroy a pathogen, small cluster of cells or even small tumors cannot be achieved [58]. In contrast, exploitation of optical excitation allows for greater heating power, for example as in ref. [62].

As mentioned, one issue with spherical gold nanoparticles is that their plasmon resonance wavelength lies well outside of the tissue window range. The problem can be addressed by using a shape such as the nanoshell or the nanorod. The optical absorption cross-sections for nanospheres of 15 nm diameter (a typical size for particles produced by the citrate [67] route) and gold nano-dogbone of 45.6 nm length, 22.5 nm diameter at mid-section are shown in Figure 3. (This latter shape can be produced by the silver/CTAB route [68]). We use it here merely as an illustrative example of the many gold nano-shapes that can exhibit a localized plasmon resonance within the tissue window.)

The thermal stability of isolated gold nanoparticles must also be considered. There will be a strong tendency for the gold shapes to coalesce into solid spheres under the action of the intrinsically high surface tension of gold, especially when heated by a laser of a resonant wavelength [69]. Change in shape, for example from a rod to a sphere, will cause the resonant wavelength of the gold particle to blue-shift, away from the tissue window and possibly away from the excitation wavelength(s) used. This is a thermally-activated process so that it will be exacerbated by higher temperatures and/or longer times. This places limits on the temperature and time-at-temperature that a gold nanorod, nanocage, nanoshell etc can be exposed to. Clearly, in individual particle mode, these special shapes would be best used in low-temperature hyperthermia mode (for which prolonged exposure is feasible) or in a once-off photothermolysis shot (which will destroy the shape of the nanoparticles). This limitation is less applicable to

solid gold spheres (since they are already in their most stable shape) although it should be noted that there will be some changes in the optical properties of gold due to lattice expansion and electron scattering as it heats up [70].

Heat generation by agglomerates of nanoparticles

The previous section highlighted the challenges of using isolated or dilute concentrations of nanoparticles for hyperthermia. On general grounds, many of these limitations can be overcome if agglomerates of many nanoparticles are used instead because local heating effects will, on balance, be increased. This is despite the fact that agglomeration induced by biological factors will decrease per particle heating efficiency due to changes in capture cross-section and, in the case of magnetic excitation, to changes in local viscosity [41].There is, however, no simple analytical solution for the heat transfer in this situation. The optical extinction cross-section of a specific arrangement of particles may be numerically calculated using the discrete dipole approximation mentioned previously but some simplifying assumptions are normally made for the heat transfer. The dimensionless optical extinction efficiency of an agglomerate is generally inferior to that of a single nanoparticle, but the key point is that the absorption cross-section in physical units is much larger. In addition, the peak extinction is red-shifted, possibly into the tissue window. For the case of gold nanospheres, this is a distinct advantage as it permits excitation at wavelengths at which they would otherwise be nearly transparent [14, 71, 72, 73, 74]. The situation is compared in Figure 4 for an isolated gold nanosphere and an agglomerate.

It is clear that the formation of the agglomerate has created optical absorption within the tissue window. In addition, the optical or magnetic properties of agglomerates are not especially sensitive to how many particles are involved once some

threshold (about ten) has been exceeded so the actual configuration of the agglomerated particles is not very important.

Of course agglomerates of magnetic nanoparticles can also be heated. Regardless of the source of excitation, an agglomeration of nanoparticles generates a volume of local heating, with each nanoparticle shedding heat into a warming volume. In practice, this strategy is attractive, as agglomerations of nanoparticles on or in a target organism or cell can be readily accomplished by some kind of chemical targeting or, in the case of macrophage targets, by the process of endocytosis [75]. Indeed, agglomeration of nanoparticles is the expected behavior in physiological fluids unless great care is taken to prevent it.

The heat transfer problem for agglomerates can be solved, at least to a first-order approximation, by allowing all absorbed energy to heat the local spherical volume of water that just envelops the agglomerate, and then estimating the transfer of that heat outward to the surrounding medium which does not contain any nanoparticles. Examples of this approach may be found in the literature [50, 57, 76]. Here we will term the volume of material that contains the nanoparticles the *active volume*, to differentiate it from the surrounding medium which does not contain any source of heat. (The same equations used for an isolated spherical nanoparticle can be used for a spherical active volume but with internal heat generation assumed to be homogeneous. The power input must be rescaled according to the density of nanoparticles present and the thermal conductivity and diffusivity of the active volume can be approximated with the values for water or human tissue.)

The active volume will begin to shed heat to the surrounding medium as soon as it starts to heat up. The temperatures that can be reached depend on the rate of heating within the active volume, on the magnitude of the heat transfer coefficient that moves

the heat out of the active volume into the surrounding medium, and, very pertinently, on the volume of the active region. Generally, however, it is assumed in the agglomerated particle scenario that the thermal payload needs to be delivered within the active volume or very close to it. In this paradigm the temperature outside of the active volume is of little importance provided that it is low enough to prevent collateral damage to the patient's healthy tissues.

An illustrative analysis for the case of laser heating is shown in Figure 5. An analogous analysis would apply in the case of heating by an agglomeration of magnetic particles within a fluctuating magnetic field. In either case, the active volume is heated by a continuous excitation (laser or magnetic field) of an intensity that will bring it to, for example, 80°C. The active volume is simultaneously being cooled by a combination of conduction and convection. Only energy deposited in the active volume is taken into account here so the actual energy flux applied may need to be larger than the values shown. In the following analysis both active volume and surrounding fluid are assumed to have the heat transfer properties of water. The equations of Pustovalov [51] have been used.

Two clinical situations are considered: destruction of a labile pathogenic organism of about 10 μm diameter to which an active volume has been attached, and destruction of solid tumor of 10 mm diameter that has been infiltrated somehow with nanoparticles (for example by extravasation or direct injection) so that the entire tumor is actually the active volume. From Figure 5(a) it is clear that the tumor can be heated with relatively modest power input whereas an appreciably more intense excitation is required to maintain the temperature of the much smaller active volume attached to a pathogen. In the latter case, convective heat transfer out of the active volume is extremely rapid due to its greater ratio of surface area-to-volume, and this is why the

much higher power input is required to maintain the temperature. Note, however, that a significantly smaller dose of energy is delivered in the case of the 'pathogen scenario' owing to the smaller active volume. For example, if the two scenarios are compared at 100 seconds, a single active volume in the pathogen scenario has delivered only 1.6×10^{-2} J of thermal energy. Of course, there would be many pathogens and hence many active volumes in the putative anti-pathogen hyperthermia. The actual total thermal energy delivered would depend on the number of active volumes within the region of excitation. If, for example, the excitation volume contained 100,000 active volumes then the total energy delivered would be much larger (1620 J). By comparison, in the case of the tumor only 162 J would have been delivered. The very high powers and energy inputs needed for the 'pathogen' or 'isolated particle' scenarios are the result of the very rapid heat transfer from nano- or micron-sized particle or active volumes. This is particularly evident if cooling following termination of the external excitation is considered, Figure 5(b). Here a heat transfer coefficient of 50 $W/m^2/K$ has been assumed (i.e. corresponding to natural convection in water). Even faster cooling would prevail if there were vascular fluid flow adjacent to the active volume [58].

Discussion: options for treating pathogens

As shown here and by others [49, 58], hyperthermia of dispersed or planktonic pathogens using magnetic excitation of isolated nanoparticles would appear to be impractical as negligible heating would be generated, even by reasonably strong alternating fields. This is due to the way heat transfer rates scale with specific surface area, and to the limited amount of energy that can be input using an alternating magnetic field. Indeed, even pathogen-sized active volumes containing *agglomerates* of magnetic nanoparticles cannot be heated to temperatures high enough to kill pathogens

if they are planktonically dispersed.

In contrast to the difficulty in targeting mobile pathogens using isolated particles, agglomerates of nanoparticles, or 'active volumes' containing a high density of nanoparticles provide a feasible strategy for pathogens due to the much greater heating power that is possible. The question is: how many nanoparticles are required per active volume at a given heating power? It is convenient to use the analytical heat transfer solution provided by Goldenburg and Trantor [44] here as this is set up in terms of a volumetric power density. We use the typical thermal conductivity (0.48 W/m/K) and thermal diffusivity (1.3×10^{-7} m^2/s) values for human tissue [77] for the medium and those of water for the active volume. We consider that heating is by gold nanospheres with a diameter of 30 nm and a Q_{ext} of 4. For illustrative purposes the results are provided for two different irradiation scenarios. These are (1) a lengthy, low power pulse that brings the active volume to a steady state temperature of 100 °C, which we designate as low-power/long-pulse (corresponding for example to a 100 mW CW laser focused to 0.5 mm diameter spot and 1.44×10^{-9} W per nanoparticle) and (2) a high power, short pulse with a power that, if allowed to continue to steady state, would eventually heat the active volume to 500°C. However, in our scenario this excitation is only applied long enough to bring the active volume to 100°C and is then terminated. We designate this as high-power/short-pulse. (This is obtainable from a pulsed laser excitation of user controllable duration and power. Since, as we will show, the fluence is much reduced under this scenario, it is permissible to apply the excitation at a higher power. Here we imagine the use of a laser of 10 W power applied to a spot of 0.5 mm diameter so that we get 1.44×10^{-7} W per nanoparticle). In both cases an active volume of the diameter indicated on the horizontal axis is considered, and the number of

nanoparticles per active volume that are required to reach 100°C under the two scenarios plotted.

As is already well-known [49, 58], it is trivial to obtain the 100°C in a large volume similar to that of a tumor, but it is more difficult to reach 100°C for pathogen-sized active volumes. Note also, that there is a geometric packing limit on how many individual nanoparticles can be closest-packed into an active volume. This constrains the power that can be produced for very small active volumes. For the conditions applied here, the high-power/short-pulse scenario is more attractive as it reaches 100°C in smaller active volumes and with fewer gold nanospheres than the alternative scenario, Figure 6(a). The fluence, or total thermal energy delivered, is the other factor to consider. This energy will be passed outwards to the surrounding tissue and should be strictly limited to prevent unnecessary collateral damage. If the active volume has a diameter of 1 μm then it takes 0.2 s to bring it to 100 °C in the low-power/long-pulse scenario but only 1.4×10^{-7} s in the high-power/short-pulse scenario. There is correspondingly a much lower fluence in the latter case notwithstanding the higher power delivered. The fluences delivered in the two scenarios are compared in Figure 6(b).

Thus far we have addressed only the two cases at opposite extremes of the hyperthermia spectrum, namely destroying macroscopic tumors or microscopic planktonic pathogens. The key insight is that very high power density is required to destroy the latter. Of course, there are other scenarios. For example, pathogens may infect localized areas such a bone, the surfaces of implants, or wounds. In these instances it would be feasible to concentrate the nanoparticles at the site of infection and, importantly, heat transfer in these cases may be constrained in some directions. This latter factor would lower the power density required to cause successful targeting.

Indeed, viable magnetic field-induced hyperthermia has already been demonstrated in certain 2D configurations [78]. There is also the possibility of treating the pathogens *ex situ.* For example, the patient's blood could be diverted to an external device in which the irradiation is performed. While a high power density of irradiation would still be required, in principle, it would be easier to control temperature in such a configuration. Another important point is that *ex situ* treatment can solve the problem of variable attenuation of the radiation source since the radiation path length can be kept short and consistent. Further research into this possibility therefore seems worthwhile.

Conclusions

It is clear that treating pathogens with nanoparticle-induced heating presents some unique challenges compared to the case of treating centimeter-sized solid tumors. The two most commonly discussed modes of excitation in this field are laser illumination of a plasmonically-resonant nanoparticle, or magnetic field excitation. The challenges are that some way must be devised to attach or assemble active volumes of nanoparticles on each pathogen, and that a rather higher excitation power must be used to maintain an effective temperature. The latter is due to the far higher ratio of surface area-to-volume of a pathogen compared to a centimeter-sized solid tumor. For example, whereas an absorbed energy of 2×10^4 W/m^2 is adequate to raise a 10 mm diameter tumor to 80°C, a 1 μm diameter pathogen requires 2×10^8 W/m^2 to achieve the same result. This latter figure is simply not available from magnetic excitation at present.

The heat payload of a nanoparticle can be delivered in the limiting cases as localized pasteurization or as a thermolysis micro-explosion. While the payload can be delivered in principle by isolated nanoparticles using optical excitation, this would only be effective in thermolysis mode. This is because in this case heating is practically

adiabatic due to the very short times involved and heat losses to the surrounding tissue can be neglected, however, very high power density is required. In contrast, heating by agglomerates of nanoparticles presents less demanding requirements for the excitation power. In the case of plasmonic-heating, allowing agglomeration of nanoparticles at the site of the pathogen brings the added advantage of increasing optical absorption cross-section within the so-called tissue 'window'.

We defined the concept of an *active volume*, a volume that contains the agglomerated nanoparticles and which can be treated as a heat source in its own right. The heat transfer characteristics for active volumes containing agglomerates were analyzed under various scenarios. Destruction of a pathogen by means of co-located active volumes is viable by optical excitation of gold nanoparticles but not by magnetic excitation. High power pulses of light with very short duration are clearly the preferred option for pathogens in order to limit the total fluence delivered, for example, pathogen-scale volumes can be raised to 100°C by a short, high power laser pulse that delivers a fluence of only 10^{-9} J per pathogen whereas a slow lower power pulse might need to be applied at 10-3 J per pathogen to achieve the same effect.

Destruction of planktonic pathogens via hyperthermia, therefore, faces strong physical challenges, and relies on extremely high power densities. It may nevertheless offer a way forward for very specialized situations, for example those that cannot be treated with antibiotics.

Acknowledgements

The authors thank their colleagues for useful discussions. DC acknowledges support

from the Australian Institute of Nuclear Science and Engineering (AINSE.

Disclosure statement

The authors declare no conflict of interest.

References

1. Thiesen B, Jordan A. Clinical applications of magnetic nanoparticles for hyperthermia. Int J Hyperthermia. 2008;24(6):467-474.
2. Cherukuri P, Glazer ES, Curley SA. Targeted hyperthermia using metal nanoparticles. Adv Drug Delivery Rev. 2010;62:339-345.
3. Kaur P, Aliru ML, Chadha AS, et al. Hyperthermia using nanoparticles – promises and pitfalls. Int J Hyperthermia. 2016;32(1):76-88.
4. Jain S, Hirst DG, O'Sullivan M. Gold nanoparticles as novel agents for cancer therapy. Bri J Radiology. 2012;85:101–113.
5. Kozissnik B, Bohorquez AC, Dobson J, et al. Magnetic fluid hyperthermia: advances, challenges, and opportunity. Int J Hyperthermia. 2013;29(8):706–714.
6. anon. MagForce AG 2017 [accessed 25th Aug 2017]. Available from: http://www.magforce.de/home.html
7. Maier-Hauff K, Ulrich F, Nestler D, et al. Efficacy and safety of intratumoral thermotherapy using magnetic iron-oxide nanoparticles combined with external beam radiotherapy on patients with recurrent glioblastoma multiforme. J Neurooncol. 2011;103:317–324.
8. E2456-06. Terminology for nanotechnology. ASTM International; 2006.
9. Moghimi SM, Hunter AC, Murray JC. Nanomedicine : Current status and future prospects. FASEB J. 2005;19:311-330.
10. Zharov VP, Mercer KE, Galitovskaya EN, et al. Photothermal nanotherapeutics and nanodiagnostics for selective killing of bacteria targeted with gold nanoparticles. Biophys J. 2006;90:619-627
11. Pissuwan D, Valenzuela S, Miller CM, et al. A golden bullet? Selective targeting of *Toxoplasma gondii* tachyzoites using antibody-functionalised gold nanoparticles. Nano Lett. 2007;7(12):3808-3812.
12. Huang W-C, Tsai R-J, Chen Y-C. Functional gold nanoparticles as photothermal agents for selective-killing of pathogenic bacteria. Nanomedicine. 2007;2(6):777-787.
13. Norman RS, Stone JW, Gole A, et al. Targeted photothermal lysis of the pathogenic bacteria, *Pseudomonas aeruginosa*, with gold nanorods. Nano Lett. 2008;8(1):302-306.
14. Pissuwan D, Valenzuela SM, Miller CM, et al. Destruction and control of *Toxoplasma gondii* tachyzoites using gold nanosphere/antibody conjugates. Small. 2009;5(9):1030-1034.
15. Kuo WS, Chang CN, Chang YT, et al. Antimicrobial gold nanorods with dual-modality photodynamic inactivation and hyperthermia. Chem Commun. 2009 (32):4853-4855.

16. Thomas LA, Dekker L, Kallumadil M, et al. Carboxylic acid-stabilised iron oxide nanoparticles for use in magnetic hyperthermia. J Mater Chem. 2009;19:6529–6535.
17. Kim M-H, Yamayoshi I, Mathew S, et al. Magnetic nanoparticle targeted hyperthermia of cutaneous *Staphylococcus aureus* infection. Ann Biomed Eng. 2013;41(3):598-609.
18. Sazgarnia A, Taheri AR, Soudmand S, et al. Antiparasitic effects of gold nanoparticles with microwave radiation on promastigotes and amastigotes of *Leishmania major* Int J Hyperthermia. 2013;29(1):79-86.
19. Levi-Polyachenko N, Young C, MacNeill C, et al. Eradicating group A streptococcus bacteria and biofilms using functionalised multi-wall carbon nanotubes. Int J Hyperthermia. 2014;30(7):490-501.
20. Chudzik B, Miaskowski A, Surowiec Z, et al. Effectiveness of magnetic fluid hyperthermia against *Candida albicans* cells. Int J Hyperthermia. 2016;32(8):842-857.
21. Pihl M, Bruzell E, Andersson M. Bacterial biofilm elimination using gold nanorod localised surface plasmon resonance generated heat. Materials Science and Engineering C. 2017;80:54-58.
22. Kalachyova Y, Olshtrem A, Guselnikova OA, et al. Synthesis, characterization, and antimicrobial activity of near-IR photoactive functionalized gold multibranched nanoparticles. ChemistryOpen. 2017;6(2):254-260.
23. Maliszewska I, Lisiak B, Popko K, et al. Enhancement of the efficacy of photodynamic inactivation of *Candida albicans* with the use of biogenic gold nanoparticles. Photochemistry and Photobiology. 2017;93(4):1081-1090.
24. Hamad-Schifferli K, Schwartz JJ, Santos AT, et al. Remote electronic control of DNA hybridization through inductive coupling to an attached metal nanocrystal antenna. Nature. 2002;415:152-155.
25. Kim D-H, Rozhkova EA, Ulasov IV, et al. Biofunctionalized magnetic-vortex microdiscs for targeted cancer-cell destruction. Nat Mater. 2010;9:165-171.
26. Weissleder R. A clearer vision for *in vivo* imaging. Nature Biotechnol. 2001;19:316-317.
27. Oldenburg SJ, Averitt RD, Westcott SL, et al. Nanoengineering of optical resonances. Chem Phys Lett. 1998;288:243-247.
28. Yu Y-Y, Chang S-S, Lee C-L, et al. Gold nanorods: electrochemical synthesis and optical properties. J Phys Chem B. 1997;101:6661-6664.
29. Jain PK, Lee KS, El-Sayed IH, et al. Calculated absorption and scattering properties of gold nanoparticles of different size, shape, and composition: applications in biological imaging and biomedicine. J Phys Chem B. 2006;110:7238-7248.
30. Harris N, Ford MJ, Mulvaney P, et al. Tunable infrared absorption by metal nanoparticles: the case for gold rods and shells. Gold Bull. 2008;41(1):5-14.
31. Lal S, Clare SE, Halas NJ. Nanoshell-enabled photothermal cancer therapy: impending clinical impact. Acc Chem Res. 2008;41(12):1842-1851.
32. Gad SC, Sharp KL, Montgomery C, et al. Evaluation of the toxicity of intravenous delivery of Auroshell particles (gold-silica nanoshells). Int J Toxicol. 2012;31(6):584-594.
33. Norregaard K, Jørgensen JT, Simón M, et al. ^{18}F-FDG PET/CT-based early treatment response evaluation of nanoparticle-assisted photothermal cancer therapy. PLoS ONE. 2017;12(5):e0177997.

34. Anselmo AC, Mitragotri S. A review of clinical translation of inorganic nanoparticles. The AAPS J. 2015;17(5).
35. Paithankar D, Hwang BH, Munavalli G, et al. Ultrasonic delivery of silica-gold nanoshells for photothermolysis of sebaceous glands in humans: nanotechnology from the bench to clinic. J Controlled Release. 2015;206:30-36.
36. Huang X, El-Sayed IH, Qian W, et al. Cancer cell imaging and photothermal therapy in the near-infrared region by using gold nanorods. J Am Chem Soc. 2006;128(6):2115-2120.
37. Ali MRK, Rahman MA, Wu Y, et al. Efficacy, long-term toxicity, and mechanistic studies of gold nanorods photothermal therapy of cancer in xenograft mice. Proc Nat Ac Sci. 2017;114(15):E3110-E3118.
38. Arnold MD, Blaber MG. Optical performance and metallic absorption in nanoplasmonic systems. Optics Express. 2009;17(5):3835-3847.
39. Atsumi T, Jeyadevan B, Sato Y, et al. Heating efficiency of magnetite particles exposed to AC magnetic field. J Magnetism Magnetic Mater. 2007;310:2841–2843.
40. Pankhurst QA, Connolly J, Jones SK, et al. Applications of magnetic nanoparticles in biomedicine. J Phys D: Appl Phys. 2003;36(13):R167–R181.
41. Périgo EA, Hemery G, Sandre O, et al. Fundamentals and advances in magnetic hyperthermia. Appl Phys Rev. 2015;2:041302.
42. Shliomis MI, Stepanov VI. In: Coffey WT, editor. Relaxation Phenomena in Condensed Matter. New York: Wiley; 1994.
43. Rosensweig RE. Heating magnetic fluid with alternating magnetic field. J Magnetism Magnetic Mater. 2002;252:370–374.
44. Goldenberg H, Tranter CJ. Heat flow in an infinite medium heated by a sphere. Br J Appl Phys. 1952;3:296-298.
45. Blanco-Andujar C, Ortega D, Southern P, et al. Real-time tracking of delayed-onset cellular apoptosis induced by intracellular magnetic hyperthermia. Nanomedicine. 2016;11(2):121–136.
46. Creixell M, Bohórquez AC, Torres-Lugo M, et al. EGFR-targeted magnetic nanoparticle heaters kill cancer cells without a perceptible temperature rise. ACS Nano. 2011;5(9):7124-712.
47. anon. MAGNABLATE I. MAGnetic NAnoparticle thermoaBLATion – Retention and Maintenance in the prostatE: A Phase 0 Study in Men London, U.K.: UCL; 2013 [accessed 26th Aug 2017]. Available from: https://www.ucl.ac.uk/surgical-interventional-trials-unit/trials/prostate/Magnablate/magnablate_I
48. Hu M, Hartland GV. Heat dissipation for Au particles in aqueous solution: relaxation time versus size. J Phys Chem B. 2002;106:7029-7033.
49. Rabin Y. Is intracellular hyperthermia superior to extracellular hyperthermia in the thermal sense? Int J Hyperthermia. 2002;18(3):194-202.
50. Skirtach AG, Dejugnat C, Braun D, et al. The role of metal nanoparticles in remote release of encapsulated materials. Nano Lett. 2005;5(7):1371-1377.
51. Pustovalov VK. Theoretical study of heating of spherical nanoparticle in media by short laser pulses. Chem Phys. 2005;308:103–108.
52. Lapotko D, Lukianova E, Potapnev M, et al. Method of laser activated nano-thermolysis for elimination of tumor cells. Cancer Letters. 2006;239:36-45.
53. Govorov AO, Richardson HH. Generating heat with metal nanoparticles. Nano Today. 2007;2(1):30-38.

54. Pissuwan D, Valenzuela SM, Killingsworth MC, et al. Targeted destruction of murine macrophage cells with bioconjugated gold nanorods. J Nanopart Res. 2007;9:1109-1124.
55. Elliott AM, Stafford RJ, Schwartz J, et al. Laser-induced thermal response and characterization of nanoparticles for cancer treatment using magnetic resonance thermal imaging. Med Phys. 2007;34(7):3102-3108.
56. Suto M, Hirota Y, Mamiya H, et al. Heat dissipation mechanism of magnetite nanoparticles in magnetic fluid hyperthermia. J Magnetism Magnetic Mater. 2009;321:1493–1496.
57. Dombrovsky LA, Timchenko V, Jackson M. Indirect heating strategy for laser induced hyperthermia: An advanced thermal mode. Int J Heat Mass Transfer. 2012;55:4688–4700.
58. Dutz S, Hergt R. Magnetic nanoparticle heating and heat transfer on a microscale: basic principles, realities and physical limitations of hyperthermia for tumour therapy. Int J Hyperthermia. 2013;29(8):790-800.
59. Harris N, Ford MJ, Cortie MB. Optimization of plasmonic heating by gold nanospheres and nanoshells. J Phys Chem B. 2006;110:10701-10707.
60. Becker M. Heat Transfer. A Modern Approach. New York: Plenum Press; 1986.
61. Draine BT, Flatau PJ. Discrete-dipole approximation for scattering calculations. J Opt Soc Am A. 1994;11(4):1491-1499.
62. Pitsillides CM, Joe EK, Wei X, et al. Selective cell targeting with light-absorbing microparticles and nanoparticles. Biophys J. 2003;84:4023-4032.
63. Letfullin RR, Joenathan C, George TF, et al. Laser-induced explosion of gold nanoparticles: potential role for nanophotothermolysis of cancer. Nanomedicine. 2006;1(4):473-480.
64. Zharov VP, Galitovsky V, Viegas M. Photothermal detection of local thermal effects during selective nanophotothermolysis. Appl Phys Lett. 2003;83(24):4897-4899.
65. Lapotko DO, Zharov VP. Spectral evaluation of laser-induced cell damage with photothermal microscopy. Lasers in Surgery and Medicine. 2005;36:22-30.
66. Stigliano RV, Shubitidze F, Petryk JD, et al. Mitigation of eddy current heating during magnetic nanoparticle hyperthermia therapy. Int J Hyperthermia. 2016;32(7):735-748.
67. Turkevich J. Colloidal gold. Part I.Historical and preparative aspects, morphology and structure. Gold Bulletin. 1985;18(3):86-91.
68. Xu X, Cortie MB. Shape change and color gamut in gold nanorods, dumbbells and dog-bones. Adv Funct Mater. 2006;16(16):2170-2176.
69. Link S, Burda C, Nikoobakht B, et al. Laser-induced shape changes of colloidal gold nanorods using femtosecond and nanosecond laser pulses. J Phys Chem B. 2000;104:6152-6163.
70. Reddy H, Guler U, Kildishev AV, et al. Temperature-dependent optical properties of gold thin films. Optic Mater Express. 2016;6(9):2776-2802.
71. Khlebtsov B, Zharov V, Melnikov A, et al. Optical amplification of photothermal therapy with gold nanoparticles and nanoclusters. Nanotechnology. 2006;17:5167-5179.
72. Nam J, Won N, Jin H, et al. pH-induced aggregation of gold nanoparticles for photothermal cancer therapy. J Am Chem Soc. 2009;131:13639-13645.
73. Hainfeld JF; Gold nanoparticles for selective IR heating Patent US 8,323,694. 2012.

74. Hainfeld JF, Lin L, Slatkin DN, et al. Gold nanoparticle hyperthermia reduces radiotherapy dose. Nanomedicine: Nanotechnology, Biology, and Medicine. 2014;10(8):1609–1617.
75. Pissuwan D, Cortie CH, Valenzuela SM, et al. Gold nanosphere-antibody conjugates for hyperthermal therapeutic applications. Gold Bull. 2007;40(2):121-129.
76. Huang X, Jain PK, El-Sayed IH, et al. Determination of the minimum temperature required for selective photothermal destruction of cancer cells with the use of immunotargeted gold nanoparticles. Photochem Photobiol. 2006;82(2):412-417.
77. Hamilton G. Investigation of the Thermal Properties of Human and Animal Tissues [PhD thesis]: University of Glasgow; 1998.
78. Coffel J, Nuxoll E. Magnetic nanoparticle/polymer composites for medical implant infection control. J Mater Chem B. 2015;3:7538-7545.

Figures

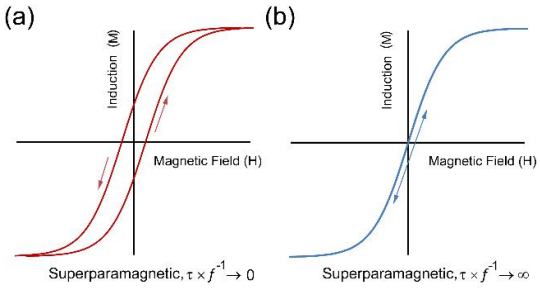

Figure 1. The magnetization versus field response of a superparamagnetic material at (a) high driving-field frequencies and (b) very low frequencies.

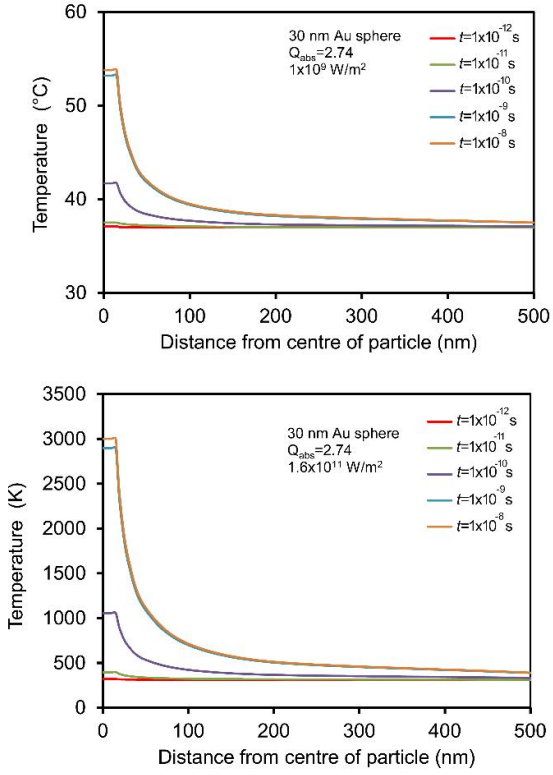

Figure 2. (a) An example of hyperthermia, obtained using a pulsed excitation intensity of 1×10^9 W/m^2. (b) An example of photothermolysis, obtained using a pulsed excitation intensity of 1.6×10^{11} W/m^2.

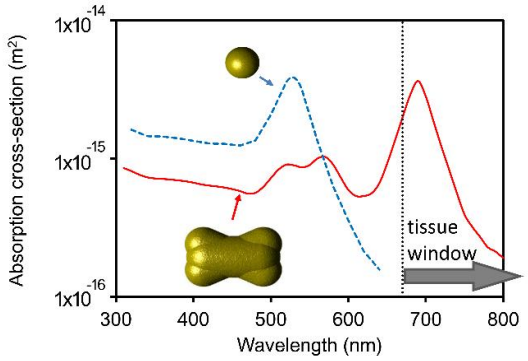

Figure 3. Calculated optical absorption efficiencies for 15 nm diameter gold nanospheres and a gold nano-dogbone with aspect ratio of 2:1.

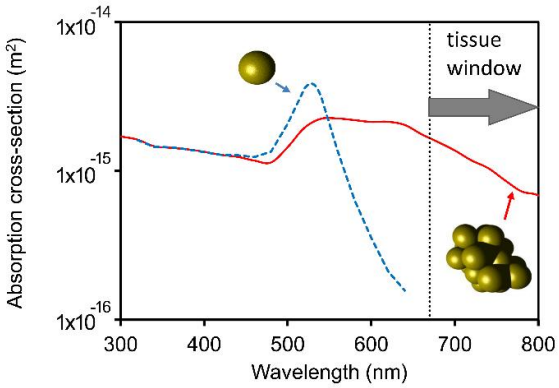

Figure 4. Optical absorption cross-sections for an isolated gold nanosphere of 15 nm diameter, and a random cluster of twenty spheres.

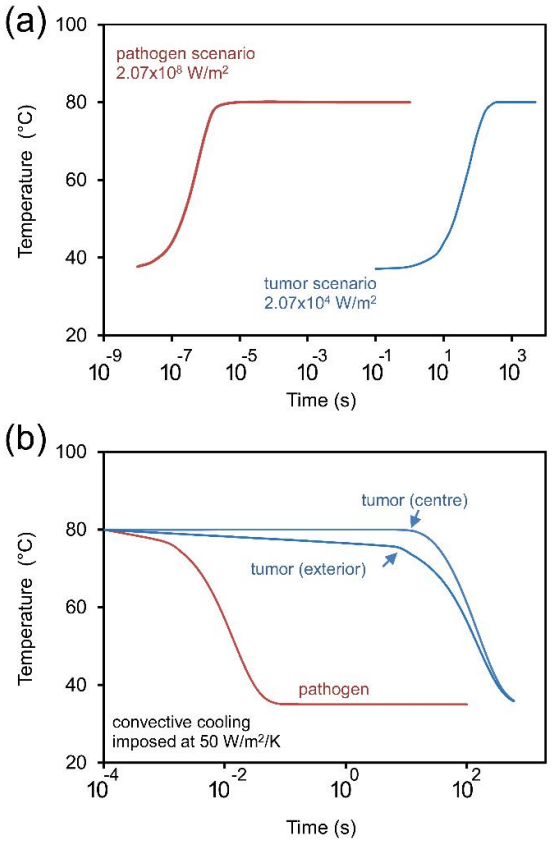

Figure 5. (a) Comparison of the time-temperature profiles when heating a 10 mm diameter tumor and a 1 μm diameter active volume (labelled as 'pathogen'). In both cases the excitation energy has been adjusted to give a steady state temperature of 80°C. (b) Comparison of the cooling profiles of the above two scenarios after excitation is terminated.

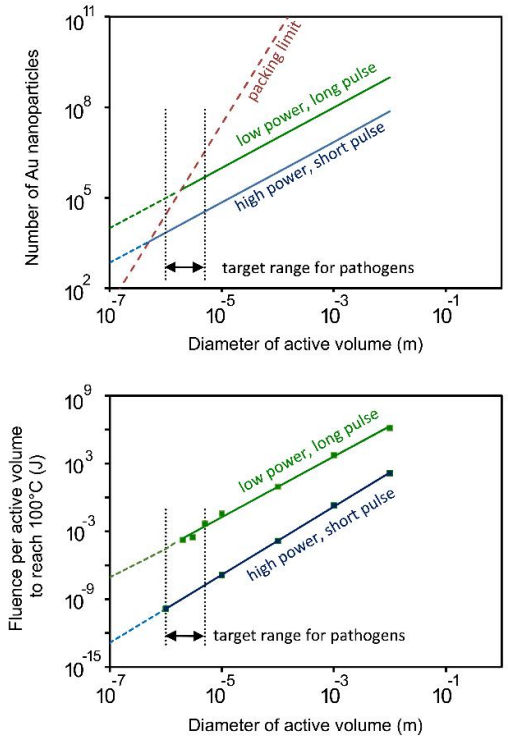

Figure 6. Comparison of the low-power/long-pulse heating scenario with the high-power/short-pulse scenario. (a) Number of nanoparticles required to achieve 100°C. (b) Total energy delivered.

Biographical notes

Prof. Michael Cortie started his career as a metallurgical engineer but now works as a physicist. He specializes in the optical properties of materials.

Dr David Cortie is a condensed-matter physicist. His interests include the magnetic properties of materials, polarized neutron scattering, and modelling of materials phenomena.

Dr Victoria Timchenko started her career with a physics degree but now practices in the domain of mechanical engineering. She specializes in the quantitative solution of fluid dynamics and heat transfer problems.